Atmos. Chem. Phys. Discuss., 9, 2823–2853, 2009
www.atmos-chem-phys-discuss.net/9/2823/2009/

Atmospheric Chemistry and Physics Discussions

This discussion paper is/has been under review for the journal *Atmospheric Chemistry and Physics (ACP)*. Please refer to the corresponding final paper in *ACP* if available.

Hydration increases the lifetime of HSO_5 and enhances its ability to act as a nucleation precursor – a computational study

T. Kurtén[1], T. Berndt[2], and F. Stratmann[3]

[1]Department of Physics, P.O. Box 64, 00014 University of Helsinki, Helsinki, Finland
[2]Leibniz-Institut für Troposphärenforschung e.V., Permoserstr. 15, 04318 Leipzig, Germany

Received: 27 November 2008 – Accepted: 17 December 2008 – Published: 28 January 2009

Correspondence to: T. Kurtén (theo.kurten@helsinki.fi)

Published by Copernicus Publications on behalf of the European Geosciences Union.

Abstract

Recent experimental findings indicate that HSO_5 radicals are likely to play a key role in the nucleation of atmospheric SO_2 oxidation products. HSO_5 radicals are metastable intermediates formed in the SO_2 oxidation process, and their stability and lifetime are, at present, highly uncertain. Previous high-level computational studies have predicted rather low stabilities for HSO_5 with respect to dissociation into SO_3+HO_2, and have predicted the net reaction HSO_3+OH → SO_3+HO_2 to be slightly exothermal. However, these studies have not accounted for hydration of HSO_5 or its precursor HSO_3. In this study, we have estimated the effect of hydration on the stability and lifetime of HSO_5 using the advanced quantum chemical methods CCSD(T) and G3B3. We have computed formation energies and free energies for mono- and dihydrates of OH, HSO_3, HSO_5, SO_3 and HO_2, and also reanalyzed the individual steps of the HSO_3+O_2→ HSO_5 →SO_3+HO_2 reaction at a higher level of theory than previously published. Our results indicate that hydration is likely to significantly prolong the lifetime of the HSO_5 intermediate in atmospheric conditions, thus increasing the probability of reactions that form products with more than one sulfur atom. Kinetic modeling indicates that these results may help explain the experimental observations that a mixture of sulfur-containing products formed from SO_2 oxidation by OH radicals nucleates much more effectively than sulfuric acid taken from a liquid reservoir.

1 Introduction

The formation of atmospheric aerosol particles by nucleation from gas-phase molecules has recently received growing experimental and theoretical interest due to the climate and health – related effects of fine particles. Despite a large number of experimental and modeling studies, little is known about the detailed molecular – scale processes behind the particle formation events observed in the atmosphere. Based on observed correlations between particle formation rates and trace gas concentrations

ACPD

9, 2823–2853, 2009

(see e.g. Riipinen et al., 2007), and also on thermodynamic classical nucleation theory calculations, nucleation in the lower troposphere has been thought to involve mainly water and sulfuric acid, with possible contributions from ions, ammonia or various organic molecules. A comparison of field measurements with laboratory experiments on sulfuric acid – ammonia – water mixtures reveals some curious discrepancies. For example, the nucleation rate typically depends on the 7th or 8th power of the sulfuric acid concentration in the laboratory experiments (Ball et al., 1999), but only on the 1st or 2nd power in the field experiments (Riipinen et al., 2007). This indicates that the critical cluster (the smallest cluster for which growth is thermodynamically more favorable than decay) in field conditions contains only 1–2 sulfuric acid molecules, as opposed to 7–8 in laboratory conditions. Also, sulfuric acid concentrations in the atmosphere during nucleation events are typically around 10^6–10^7 molecules cm^{-3}, while the threshold concentration for nucleation in laboratory experiments is around 10^{10} molecules cm^{-3}.

Recently, Berndt et al. (2005, 2006, 2007) compared the nucleation rates of sulfuric acid formed from SO_2 oxidation by OH radicals to that of sulfuric acid taken from a liquid reservoir. They found that the threshold H_2SO_4 concentration for particle formation was 10^7 molecules cm^{-3} if H_2SO_4 was produced in situ via the reaction of OH radicals with SO_2 in the presence of water vapor, and 10^{10} molecules cm^{-3} if the H_2SO_4 was taken from a liquid reservoir or produced in situ via the reaction of SO_3 with water vapor. Other experimental findings confirm a H_2SO_4 threshold concentration of about 10^7–10^8 molecules cm^{-3} (Burkholder et al., 2007; Young et al., 2008; Benson et al., 2008) when produced in situ from SO_2. It should be noted that the differences regarding the stated threshold H_2SO_4 concentrations reported from various studies are probably caused by the different experimental conditions used.

Sulfuric acid production from SO_2 oxidation proceeds via a series of radical reactions. First, SO_2 reacts with an OH radical, which is normally produced from water vapor via reaction with electronically excited atomic oxygen $O(^1D)$, which in turn is formed from ozone photolysis. (Alternatively, the OH radical can be formed from ozonolysis of

ACPD
9, 2823–2853, 2009

an alkene in a dark reaction.)

$$SO_2 + OH + M \rightarrow HSO_3 + M \quad \text{(R1)}$$

Where M denotes a collision partner (typically N_2 or O_2). The HSO_3 radical then rapidly reacts with molecular oxygen to yield either SO_3 and HO_2 or an intermediate complex HSO_5:

$$HSO_3 + O_2 \rightarrow SO_3 + HO_2 \quad \text{(R2a)}$$

$$HSO_3 + O_2 + M \rightarrow HSO_5 + M \quad \text{(R2b)}$$

SO_3 reacts with water (catalyzed by another water molecule) to yield sulfuric acid:

$$SO_3 + 2H_2O \rightarrow H_2SO_4 + H_2O \quad \text{(R3)}$$

The HSO_5 radical may also decompose to SO_3 and HO_2, or it may react with other compounds. For example, self-reaction would form peroxodisulfuric acid, $H_2S_2O_8$:

$$HSO_5 \rightarrow SO_3 + HO_2 \quad \text{(R4)}$$

$$HSO_5 + HSO_5 \rightarrow H_2S_2O_8 + O_2 \quad \text{(R5)}$$

If Reaction (4) is very rapid, Reactions (2a) and (2b) can not necessarily be distinguished from each other. At present, it is not known if the direct Reaction (2a) is possible, or if the reaction always proceeds via a transient HSO_5 intermediate. Various authors (Davis et al., 1979; Wayne, 2000) have suggested that HSO_5 in atmospheric conditions is likely to be hydrated, but to our knowledge no experimental or computational evidence of this has been presented prior to this study.

The HSO_3+O_2 reaction has been investigated by several groups. In a computational study, Majumdar et al. (2000) proposed that the reaction proceeds via three steps:

$$HSO_3 + O_2 \rightarrow HSO_5(R) \quad \text{(R2c)}$$

ACPD
9, 2823–2853, 2009

$HSO_5(R) \rightarrow HSO_5(TS)$ (R2d)

$HSO_5(TS) \rightarrow HSO_5(P)$ (R2e)

$HSO_5(P) \rightarrow SO_3 + HO_2$ (R2f)

Where $HSO_5(R)$ is a reactant complex corresponding to $HSO_3 \bullet O_2$ ($HOSO_2 \bullet O_2$), $HSO_5(P)$ is a product complex corresponding to $SO_3 \bullet HO_2$, and $HSO_5(TS)$ is a transition state connecting the two, where the H-atom is shared by the S-O-O and S-O groups.

Very recently, Berndt et al. (2008) and Laaksonen et al. (2008) have discussed the implications of the experimental results in terms of these mechanisms, and concluded that a nucleation mechanism involving HSO_5 or its reaction products is likely to explain nucleation starting from $OH+SO_2$ observed in atmosphere as well as in the laboratory. Salonen et al. (2009) have investigated the stability of clusters of sulfuric acid together with various intermediate and alternative products of the SO_2 oxidation chain, and concluded that while HSO_5 itself is unlikely to nucleate very effectively, a mixture of sulfuric acid and HSO_5 reaction products containing more than one sulfur atom (such as peroxodisulfuric acid) are likely to nucleate more effectively than sulfuric acid on its own.

A crucial uncertainty in the proposed nucleation mechanism is the lifetime of HSO_5 especially with respect to dissociation via path (4) or (2f). Based on computational and experimental studies (Stockwell and Calvert, 1983; Li and McKee, 1997), the dissociation of HSO_5 into SO_3 and HO_2 could be very rapid. Thus, the fraction of HSO_5 molecules that live long enough to collide with other sulfur-containing molecules would be small, and any nucleation mechanism starting from HSO_5 would be inefficient. However, previous computational studies have neglected the effect of water vapor, which is always present in both laboratory and field studies in concentrations far exceeding those of all sulfur – containing molecules combined. In principle, hydration could increase the steady-state concentration of HSO_5, and thus the probability of bimolecular reactions involving HSO_5, by four different mechanisms:

ACPD
9, 2823–2853, 2009

(1) Thermodynamic stabilization of HSO_5 with respect to the products SO_3 and HO_2.

(2) Thermodynamic stabilization of HSO_5(R) with respect to HSO_5(P).

(3) Kinetic stabilization of HSO_5(R) with respect to HSO_5(P), i.e. the barrier for Reaction (2d) above could be increased by hydration.

(4) Increasing the fraction of HSO_3+O_2 collisions that lead to HSO_5 formation as opposed to direct SO_3+HO_2 formation (if the latter is at all possible). E.g. if HSO_3 were hydrated in Reactions (2a/2b), there would be more vibrational degrees of freedom to accommodate the excess energy liberated in the reaction, and thus a greater degree of energy accommodation, and a higher probability for the transiently formed reaction complex to stay together.

Mechanism number 3 is not very likely, as water typically tends to catalyze proton transfer reactions rather than hindering them. In this study, we have assessed the effect of mechanisms 1 and 2 above using advanced quantum chemical methods, and found them both to be significant.

2 Computational details

We have computed free energies of formation for SO_2, OH, HSO_3, O_2, HSO_5, SO_3 and HO_2 molecules and most of their mono- and dihydrates. (The hydrates of O_2 were not studied, as they are likely to be extremely weakly bound due to the nonpolarity of the O_2 molecule. Also, only the monohydrate of SO_2 was considered, as experimental evidence (Dermota et al., 2005) indicates that SO_2 in water clusters only interacts with one water molecule.) Free energies have been computed using the G3B3 combination method (Baboul et al., 1999) which involves B3LYP/6-31G(d) geometry optimizations and frequency calculations (using a scaling factor of 0.96) together with a series of higher-level (MP2(full), MP4 and QCSID(T)) single-point energy calculations and empirical corrections. Assuming certain additivity rules, the G3B3 energy is a reasonable

estimate of the QCISD(T)(full) energy with a large triple-zeta basis set. For a sample set of 299 data points (Baboul et al., 1999), the mean absolute deviation of the energies predicted by the G3B3 method is 0.99 kcal/mol. Some calculations have also been performed with the G2 combination method (Curtiss et al., 1991), which is similar to G3B3 except that frequencies are computed at the HF/6-31G(d) level and geometries at the MP2/6-31G(d) level. Unfortunately, most of the G2 calculations on hydrated HSO_5 failed as the MP2 geometry optimizations did not converge. This may be related to the finding by Majumdar et al. (2000) that the MP2 method does not always yield reliable results (especially structures or vibrational frequencies) for all configurations of the HSO_5 system. To assess the reliability of the G3B3 values (and also to compute more reliable estimates for the reaction energetics than published in earlier studies), we further optimized the structures of the free molecules, monohydrates and selected dihydrates at the UB3LYP/6-311++G(3df,3pd) level (Becke, 1993; Lee et al., 1988) and performed UCCSD(T)/6-311++G(3df,3pd) and UCCSD(T)/aug-cc-pV(T+d)Z (Knowles et al., 1993; Deegan and Knowles, 1994) single-point energy calculations at these geometries. (The aug-cc-pV(T+d)Z basis set is identical to the standard aug-cc-pVTZ basis set for first- and second- row atoms, and contains an extra d – orbital for third-row atoms, as this has been shown to yield more accurate atomization energies, see Dunning et al., 2001). Due to the extreme computational cost and prohibitive scaling of the UCCSD(T) method, we were unable to treat the HSO_5 dihydrate clusters at this level.

To maintain consistency with G3B3 thermochemical parameters, a scaling factor of 0.967 was used in calculating the thermal entropy and enthalpy contributions at the UB3LYP/6-311++G(3df,3pd) level. This was based on data for the 6-311+G(3df,2p) basis set from the Computational Chemistry Comparison and Benchmark Database (http://cccbdb.nist.gov/default.htm). This scaling factor was based on 3448 individual vibrational frequencies from 308 different molecules. A slightly larger scaling factor of 0.970 was given for the basis set 6-311+G(3df,2pd), which is closer in size to the basis used in this work. However, as this value was not based on direct calculations,

but on comparisons with B3LYP/cc-pVTZ calculations, we chose the former value as somewhat more reliable. This is partly supported by a recent study by Anderson and Uvdal (2005), in which a scaling factor of 0.9679 was recommended for B3LYP calculations with all Pople basis sets larger than 6-311++G(d,p). In any case, the difference between results obtained with the three scaling factors (0.967, 0.9679 and 0.970) are minimal. All thermochemical parameters presented here have been computed using the rigid rotor and (scaled) harmonic oscillator approximations.

SO_2•H_2O, OH•$(H_2O)_n$, HSO_3•H_2O, SO_3•$(H_2O)_n$ and HO_2•$(H_2O)_n$ (with n=1, 2, . . .) clusters have been computationally studied previously (Li and McKee, 1997; Du et al., 2006; Aaltonen and Fransisco, 2003; Fliegl et al., 2006; Larson et al., 2000; Alongi et al., 2006), and initial geometries for these systems were taken from the published literature. To our knowledge, there are no previous studies on HSO_3•$(H_2O)_2$ or HSO_5•$(H_2O)_{1...2}$ clusters. For these systems, initial guesses were generated using the Spartan program (Wavefunction Inc, 2002), and pre-optimized at the B3LYP/6-31G(d) level (and for some clusters also at the PBE/6-31+G(2d,p) level with density fitting). For the HSO_5 mono- and dihydrates, several of the initial guess geometries failed to converge at the B3LYP and PBE levels, and only a few structures could finally be used for the higher-level calculations. UCCSD(T) calculations were performed using the Molpro 2006.1 program (Werner et al., 2006), some RI-MP2 test calculations (Weigend and Häser, 1997; Weigend et al., 1998) were performed on Turbomole 5.10 (Alrichs et al., 1989), and all other calculations were carried out using the Gaussian 03 program suite (Frisch et al., 2004). The default energy and geometry convergence criteria for each program were used in all calculations. It should be noted that for the HSO_5(TS) and HO_2 systems, both of which belong to the point group Cs, using the default symmetry settings of the Molpro program causes severe errors in the computed reaction energies, as the calculation then corresponds to an excited electronic state (with symmetry ^{2}A'). To compute the energy for the ground state (with symmetry ^{2}A"), the symmetry of the ground-state wavefunction must either be explicitly specified (using the wf and occ keywords), or the calculation must be performed without using symmetry (keyword

ACPD
9, 2823–2853, 2009

nosym). A similar phenomenon occurs for the OH radical.

The Cartesian co-ordinates and energetics of all studied structures are given in the supporting information (http://www.atmos-chem-phys-discuss.net/9/2823/2009/acpd-9-2823-2009-supplement.pdf).

3 Results and discussion

3.1 HSO_3+O_2 reaction energetics

Previous studies have found the net reaction HSO_3+O_2→ SO_3+HO_2(2a) to be either exothermic (Li and McKee, 1997; Klopper et al., 2008), weakly endothermic (Majumdar et al., 2000) or strongly endothermic (Benson, 1978; Nagase et al., 1988). Experimentally, the reaction is known to be the exclusive fate of HSO_3 in the atmosphere with a rate constant of 4.3×10^{-13} cm^3 $molecule^{-1}$ s^{-1} at 293 K (Gleason et al., 1987; Gleason and Howard, 1988). The experimental results thus indicate that the studies predicting a strong endothermicity are likely to be in error. The reaction energetics predicted for this reaction at various levels of theory are given in Table 1. (Note that several more basis sets were used in the study by Majumdar et al. 2000; the rest of their values lie between those presented here.)

It can be seen from Table 1 that while B3LYP and MP2 calculations predict the reaction to be strongly endothermic unless very large basis sets are used, the more advanced methods including high-level correlation (G2, G3B3, UCCSD(T)) predict the reaction energy and enthalpy to be slightly below, though quite close to, zero. The reaction free energies predicted by the more advanced methods lie on both sides of zero, and are all quite small. The large differences between MP2 or DFT energies on one hand and G2, G3B3 or coupled-cluster energies on the other indicates that high-level electron correlation plays a central role in the energetic of the reaction, as noted by Majumdar et al. (2000). The difference between the G3B3, UCCSD and UCCSD(T) energies (as well as the UCCD and UCCSD(T) energies using two different basis sets)

are of the same size as the predicted endo- or exothermicity, indicating that a quantitatively reliable prediction of the sign of the energy change of the reaction likely requires even more advanced methods than those used here. In a very recent state-of-the-art computational study, Klopper et al. (2008) recalculated the heat of formation of HSO_3 using a combination of very high-level methods, and applied this data to estimate the enthalpy of Reaction (2a), finding it to be weakly exothermic. Our best results are in fairly good agreement with their enthalpy value of −2.3±0.7 kcal/mol. Comparing the free energy and enthalpy values, we can conclude that also the free energy change of the reaction is very likely to be slightly below zero.

To our knowledge, only Majumdar et al. (2000) have previously addressed the detailed energetics of all the elementary reaction steps 2c–2f. The study by Nagase et al. (1988) contains data for Reaction (2c), while that of Solimannejad et al. (2004) contains data for Reaction (2f). The energetics of these individual steps are reported in Table 2. The structure of the molecules HSO_3, HSO_5(R), HSO_5(TS) and HSO_5(P) are shown in Fig. 1. The structures are drawn using the MOLEKEL 4.3 visualization package (Portmann, 2002).

As for the net Reaction (2a), there are considerable differences between the different methods. Compared to the more advanced G2, G3, G3B3 and coupled-cluster methods, MP2 and B3LYP significantly underestimate the binding energy of HSO_5(R) and the barrier height for the HSO_5(R)→HSO_5(P) conversion. However, the energetics for Reaction (2f) predicted by the different methods are relatively similar.

Regardless of the method used, the HSO_5(TS) transition state is predicted to be lower in electronic energy and enthalpy than the reactants HSO_3+O_2. On the other hand, all methods except G2 predict the transition state to lie higher in free energy than the free reactant molecules. The highest-level (UCCSD(T)/aug-cc-pV(T+d)Z//UB3LYP/6-311++G(3df,3pd)) ΔG value for the HSO_3+O_2→→ HSO_5(TS) free energy change is +0.77 kcal/mol, indicating that, as for the net Reaction (2a), the value is likely to be close to zero, and even more advanced methods would be needed to reliably determine the sign of the free energy difference. Nevertheless, it is clear

from the higher-level data that net barrier for the $HSO_3+O_2 \rightarrow\rightarrow HSO_5(P)$ process is unlikely to be larger than a few kcal/mol, which supports the experimental observations (Gleason et al., 1987; Gleason and Howard, 1988) that the reaction should be reasonably fast at ambient temperatures.

4 Effect of hydration

Table 3 shows the formation energetics of $X{\bullet}H_2O$ and $X{\bullet}(H_2O)_2$ clusters computed at various levels of theory, with X=SO_2, OH, HSO_3, $HSO_5(R)$, $HSO_5(P)$, SO_3 and HO_2. For simplicity, only G3B3 and UCCSD(T)/aug-cc-pV(T+d)Z//UB3LYP/6-311++G(3df,3pd) results are given from this work, see the supporting information for lower-level coupled-cluster values. The minimum-energy structures of the hydrated clusters are shown in Fig. 2. (The structures correspond to the B3LYP/6-31G(d) geometries used in the G3B3 calculations, since these are available for all structures. Qualitatively, these were in most cases – see below for the single major exception – very similar to the UB3LYP/6-311++G(3df,3pd) geometries computed for some of the clusters. See the supporting information for all computed Cartesian co-ordinates.)

For the molecules for which previous data on hydrates are available (SO_2, OH, HSO_3, SO_3 and HO_2), our results are in fairly good agreement with previous studies. It should especially be noted that the binding energy predicted for the $OH{\bullet}H_2O$ complex using the UCCSD(T)/aug-cc-pVTZ single-point energy computed at the UB3LYP/6-311++G(3df,3pd) geometry is within 0.005 kcal/mol of that computed by Du et al. (2006) using a full RCCSD(T)/aug-cc-pVTZ geometry optimization. This indicates that the errors induced by the DFT geometry optimization for our hydrated radical complexes are likely to be relatively minor, at least if the basis set is large enough. Similarly, it should be noted that our hydration enthalpies for HO_2 are all within the error margins of the experimental result by Kanno et al. (2006), and that our best value for the $SO_3{\bullet}H_2O$ binding energy is within the estimated error margins of that computed by Fliegl et al. (2006) using a combination of very advanced methods. The G3B3 and

UCCSD(T)/aug-cc-pV(T+d)Z//UB3LYP/6-311++G(3df,3pd) values are also in reasonable agreement with each other, except for the $HSO_5(R)•H_2O$ cluster, for which the coupled-cluster binding energy is almost 3 kcal/mol less than the G3B3 binding energy. (The difference in free energies is only about 1.2 kcal/mol.) The reason for this difference may be the fact that, as pointed out by Majumdar et al. (2000), the geometries predicted at the B3LYP level using double- and triple-zeta basis sets (6-31G(d,p) and TZ2P++ in their case) differ quite significantly from each other with regard to the SOH...OOS distance. With the smaller basis sets, the distance is predicted to be rather short (1.71 and 1.75 Å for the 6-31G(d,p) and 6-31G(d) basis sets, respectively), corresponding to an intramolecular hydrogen bond, whereas calculations with a large basis set predict the distance to be much larger (2.74 for both the TZ2P++ and 6-311++G(3df,3pd) basis sets). Presumably, the B3LYP calculations with larger basis sets correspond at least somewhat better to the high-level wavefunction-based methods employed in the G3B3 and CCSD(T) energy calculations, as indicated by the excellent agreement for the $OH•H_2O$ cluster mentioned above. Thus, the high $HSO_5(R)•H_2O$ binding energy found at the G3B3 level is probably slightly overestimated, as the B3LYP/6-31G(d) geometry for $HSO_5(R)$ used in the calculation is likely to be unfavorable for the higher-level methods.

Regardless of the method used, it can be seen from Table 3 that SO_2 and OH are only weakly bound to water, while SO_3 and HO_2 are moderately and HSO_3 and HSO_5 strongly hydrated. Especially the reactant complex $HSO_5(R)$ is very strongly bound to water, even after the probable overbinding in the G3B3 energies is accounted for. Hydration by one water molecule stabilizes the reactant form of HSO_5 by around 3–5 kcal/mol compared to the product form, while both HSO_5 dihydrates are more strongly bound than any of the other dihydrate clusters. However, the difference in hydration energies between the dihydrates $HSO_5(P)•(H_2O)_2$ and $HSO_5(R)•(H_2O)_2$ is only around 1–2 kcal/mol, less than half of the difference between the monohydrates. The reason for this is apparent from Fig. 2i): the $HSO_5(P)•(H_2O)_2$ minimum-energy structure actually corresponds to an ion pair cluster $SO_5^-•H_3O^+•H_2O$. (Other, local minima without

proton transfer were also found at the G3B3 level, but they were all less stable than the ion pair structure by several kcal/mol. See the supporting information for their Cartesian co-ordinates.) As the SO_5^- radical ion is known to be an effective oxidant in aqueous solutions (Wayne, 2000; Das, 2001) this prediction, if true, would have significant implications for the reactivity and nucleating potential of hydrated HSO_5. For example, two SO_5^-•H_3O^+•H_2O clusters could be expected to react rapidly to yield $S_2O_8^{2-}$•$(H_3O^+)_2$•$(H_2O)_2$+O_2, and the resulting $H_2S_2O_8$ cluster can then be expected to nucleate more efficiently than pure sulfuric acid (as discussed by Salonen et al., 2009). Furthermore, SO_5^- is known to be a strong oxidant for sulfite in aqueous solutions (Das, 2001). By analogy, SO_5^-•H_3O^+•H_2O or the higher hydrates SO_5^-•H_3O^+•$(H_2O)_y$ (y=2, 3, ...) can efficiently oxidize further SO_2 picked up from the gas phase. This process leads to growth of the initial HSO_5 hydrates.

However, the B3LYP/6-31G(d) method used for geometry optimizations within the G3B3 combination approach is rather modest, and the predicted ion pair structure could be an artifact. To check if this is the case, we performed further geometry optimizations on the HSO_5(P)•$(H_2O)_2$ cluster at the UB3LYP/6-311++G(3df,3pd), UMP2/6-311++G(2d,2p) and RI-MP2/aug-cc-pV(T+d)Z levels. The UB3LYP/6-311++G(3df,3pd) optimization also led to an ion pair structure, while the UMP2/6-311++G(2d,2p) and RI-MP2/aug-cc-pV(T+d)Z optimizations led to structures where the hydrogen atom was equally shared between the S-O-O and OH_2 groups. We then computed the G3B3 single-point electronic energies at these geometries, and found them to be 0.55 kcal/mol higher and 0.32 lower than that computed at the UB3LYP/6-31G(d) minimum geometry, for the UMP2/6-311++G(2d,2p) and RI-MP2/aug-cc-pV(T+d)Z methods, respectively. (It should be noted that the G3B3 method is parametrized to the B3LYP/6-31G(d) geometries, so the accuracy of these single-point energy calculations may not be as good as that of the original G3B3 method. However, they should still be good indications of the higher-level potential energy surface.) Given the influence of higher-level correlation on the reaction energetics of the HSO_5 system (see e.g. Tables 2–3), neither the B3LYP nor the MP2 structures are likely to

ACPD
9, 2823–2853, 2009

be totally trustworthy. Ideally, geometry optimizations would need to be performed at e.g. the UCCSD(T)/aug-cc-pV(T+d)Z level to determine how many water molecules are needed to induce proton transfer from HSO_5 to H_2O. Unfortunately, this is beyond the capabilities of present computer hardware. Still, the fact that both B3LYP and MP2 methods predict at least a partial proton transfer for the $HSO_5(P)\bullet(H_2O)_2$ cluster is a strong indication that the minimum-energy geometry for $HSO_5(P)\bullet(H_2O)_2$ is likely to have at least some degree of an ion-pair character.

Using the data in Table 3, the influence of hydration on the net Reaction (2a) and the dissociation Reaction (2f) can now be estimated. G3B3 and UCCSD(T)/aug-cc-pV(T+d)Z//UB3LYP/6-311++G(3df,3pd) reaction energy and free energy values for Reactions (2a), (2c)+(2d) and (2f) with one or more of the participating species hydrated are given in Table 4. Reaction pathways including the dissociation of water from the clusters were not included in the table as they are all predicted to be strongly endothermal.

A comparison of Table 4 with Tables 1 and 2 demonstrate that hydration does indeed stabilize HSO_5 via both mechanisms 1 and 2 presented in the Introduction. E.g. the $HSO_5(R) \rightarrow HSO_5(P)$ conversion is predicted to have a ΔG of 3.39 kcal/mol at the UCCSD(T)/aug-cc-pV(T+d)Z//UB3LYP/6-311++G(3df,3pd) level, increasing to 6.81 kcal/mol after hydration by one water molecule. (Corresponding values for the G3B3 method are 0.08, 4.67 and 1.36 kcal/mol for zero, one and two water molecules, respectively, the latter low value being due to the predicted ion pair formation.) Similarly, the free energy values for the most favorable routes for the net Reaction (2a) at the same level are 1.60 kcal/mol and 2.20 kcal/mol after hydration by one and two water molecules, respectively, compared to −0.26 kcal/mol for the unhydrated reaction. (Corresponding G3B3 values are −1.76, −1.08 and 0.51 kcal/mol, for zero, one and two waters, respectively). While the difference is relatively small – about 2 kcal/mol – the effect on the equilibrium constant for the reaction is significant, and hydration is likely to strongly increase the lifetime of HSO_5 in ambient conditions. If the prediction of an ion pair structure for $HSO_5(P)\bullet(H_2O)_2$ is correct, then the monohydrate will be sta-

ACPD
9, 2823–2853, 2009

bilized mainly by mechanism 1 (stabilization with respect to the $HSO_5(R) \rightarrow HSO_5(P)$ conversion) while the dihydrate (and, presumably, higher hydrates) will be stabilized mainly by mechanism 2 (stabilization with respect to dissociation into SO_3+HO_2). The dominant stabilization mechanism would then dependent on the relative humidity (RH). If, on the other hand, the prediction of an ion pair structure is incorrect, then mechanism 1 is likely to dominate both for the mono- and dihydrates. It should be noted that the net reactions $HSO_5(R)\bullet(H_2O)_2 \rightarrow\rightarrow SO_3\bullet(H_2O)_x+HO_2\bullet(H_2O)_{2-x}$ (x=0,1,2) are in any case all strongly endothermal, independent of the prediction of proton transfer for $HSO_5(P)\bullet(H_2O)_2$. Also, possible errors in the configurational sampling of HSO_5 hydrates (i.e. the minimum-energy geometries described here may not be the global minima) would only serve to further increase the stability of these structures with respect to hydrated SO_3 and HO_2.

4.1 Kinetic modeling and atmospheric implications

The data in Tables 3 and 4 unequivocally show that if HSO_5 clusters are hydrated, they will be significantly stabilized both with respect to the $HSO_5(R) \rightarrow HSO_5(P)$ conversion and with respect to dissociation into SO_3+HO_2. The key question that then remains is the mechanism by which HSO_5 can be hydrated in the first place. If only a fraction of unhydrated HSO_3+O_2 collisions lead to the formation of HSO_5, then HSO_5+H_2O collisions are not likely to be an effective source of hydrated HSO_5, especially given the presumably short lifetime of unhydrated HSO_5. The major source of water molecules is thus likely to be the hydration of the preceding reactants in the SO_2 oxidation chain. O_2 is unlikely to be hydrated due to the lack of a dipole moment, and as shown in Table 3, SO_2 is only weakly bound to water. OH is somewhat more strongly hydrated, but using the UCCSD(T)/aug-cc-pV(T+d)Z//UB3LYP/6-311++G(3df,3pd) free energy of hydration at 298 K together with a H_2O concentration of 0.015488 atm (corresponding to RH 50% at 298K) in the law of mass action leads to the conclusion that less than 0.1% of OH molecules will be bound to water at equilibrium. Thus, the only remaining possibility is the hydration of HSO_3. The free energy changes in Table 3 are large enough that

a significant fraction (on the order of 10–20%) of HSO_3 molecules are bound to water at equilibrium in ambient conditions.

We have performed kinetic modeling to determine whether or not these equilibria have enough time to form hydrated HSO_3 and subsequently hydrated HSO_5, in the experimental setup of Berndt et al. (2005, 2006, 2008), as well as in the atmosphere. In order to do this, the UCCSD(T)/aug-cc-pV(T+d)Z//UB3LYP/6-311++G(3df,3pd) Gibbs free energy changes for the $HSO_3+H_2O \rightarrow HSO_3\bullet(H_2O)$ and $HSO_3\bullet(H_2O)+H_2O \rightarrow HSO_3\bullet(H_2O)_2$ reactions were recomputed at the experimental temperature of 293 K, yielding values of −2.083 and −1.237 kcal/mol, respectively. These correspond to equilibrium constants of 1.429×10^{-18} cm^3 molecule^{-1} and 3.341×10^{-19} cm^3 molecule^{-1}, respectively.

The following reaction scheme was used for a more detailed description of the processes going on in the course of SO_2 oxidation by OH using as the OH source the photolysis of O_3, as applied in the IFT-LFT experiments (Berndt et al., 2005, 2006):

$$O_3 \rightarrow \ldots \rightarrow 2OH \quad \text{(M1)}$$

$$OH + CO \rightarrow \text{products} \quad \text{(M2)}$$

$$OH + SO_2 \rightarrow HSO_3 \quad \text{(M3)}$$

$$HSO_3 + O_2 \rightarrow HSO_5 \quad \text{(M4)}$$

$$HSO_3 + H_2O \rightarrow HSO_3\bullet H_2O \quad \text{(M5)}$$

$$HSO_3\bullet H_2O \rightarrow HSO_3 + H_2O \quad \text{(M6)}$$

$$HSO_3\bullet H_2O + O_2 \rightarrow HSO_5\bullet H_2O \quad \text{(M7)}$$

$$HSO_3\bullet H_2O + H_2O \rightarrow HSO_3\bullet(H_2O)_2 \quad \text{(M8)}$$

$$HSO_3\bullet(H_2O)_2 \rightarrow HSO_3\bullet H_2O + H_2O \quad \text{(M9)}$$

$HSO_3•(H_2O)_2 + O_2 \rightarrow HSO_5•(H_2O)_2$ (M10)

Simulations have been carried out using the following rate constants. (Note that the degree of hydration of HSO_3 is independent of rate constants k_{M1}... k_{M3}). For the reaction of all $HSO_3•(H_2O)_x$ species with O_2, the rate constant for the unhydrated molecule $k_{M4}=k_{M7}=k_{M10}=4.3\times10^{-13}\,cm^3\,molecule^{-1}\,s^{-1}$ (Gleason et al., 1987; Gleason and Howard, 1988) was used. For addition of water, rate constants of $k_{M5}=k_{M8}=10^{-10}\,cm^3\,molecule^{-1}\,s^{-1}$ (close to the diffusion limit) were used, and for the dissociation reactions the values corresponded to the equilibrium constants: $k_6=7\times10^7\,s^{-1}$ and $k_9=3\times10^8\,s^{-1}$. The relative humidity was set to 22%, based on the most common RH in the experiments (corresponding to $[H_2O]=1.24\times10^{17}\,molecule\,cm^{-3}$ at 293 K), and $[O_2]$ was set to $4.92\times10^{18}\,molecule\,cm^{-3}$ (synthetic air). In these conditions, we find that SO_2 is converted to 84.9% HSO_5, 14.6% $HSO_5•H_2O$ and 0.5% $HSO_5•(H_2O)_2$. Even for conditions with $[O_2]=2.46\times10^{17}\,molecule\,cm^{-3}$ (1 vol% O_2 in N_2, as applied in the experiments reported in Berndt et al., 2005) at RH=22 %, the yields are nearly unchanged; 84.4% HSO_5, 15% $HSO_5•H_2O$ and 0.6% $HSO_5•(H_2O)_2$. This very simple model neglects the hydration equilibria of HSO_5. Assuming that the decomposition of unhydrated HSO_5 to HO_2 and SO_3 is more effective than the reaction with water and, on the other hand, $HSO_5•H_2O$ and $HSO_5•(H_2O)_2$ are relatively stable with respect to decomposition, about 15% of reacted SO_2 can produce nucleation precursors other than H_2SO_4 at RH=22 %. With increasing relative humidity, this model predicts increasing yields of hydrated HSO_5. For RH=80 % it follows that 58.6% HSO_5, 36.4% $HSO_5•H_2O$ and 5% $HSO_5•(H_2O)_2$ are formed in the SO_2 oxidation.

$HSO_5•H_2O$, $HSO_5•(H_2O)_2$ or higher hydrates can be treated as potential nucleation precursors reacting, for instance, in a self-reaction, or oxidizing further SO_2 after picking it up from the gas phase. For example, if the prediction of an ion pair structure of $HSO_5(P)•(H_2O)_2$ is correct, then the self-reaction of this species is likely to proceed with

ACPD
9, 2823–2853, 2009

little or no barrier like the self-reaction of sulfamic acid (Lovejoy and Hanson, 1996):

$$HSO_5\bullet(H_2O)_2 + HSO_5\bullet(H_2O)_2 \rightarrow \ldots \rightarrow \text{nuclei} \quad \text{(M11)}$$

Using an order-of-magnitude estimate of $k_{M11}=1\times10^{-10}$ cm^3 molecule^{-1} s^{-1} for the rate constant of the $HSO_5\bullet(H_2O)_2$ ion pair self-reaction, and assuming that only this step is responsible for critical cluster formation, the rate at which the reaction products are produced via path (M11) is slightly larger than the formation rate of detected particles measured for commonly used conditions in the laboratory experiments (Berndt et al., 2005, 2006, 2008). Further addition of $HSO_5\bullet(H_2O)_2$ or $HSO_5\bullet H_2O$, and/or other SO_2 oxidation to the produced clusters could govern the growth process.

This rough estimate is affected by a few assumptions, some of which require further research. It shows, however, that the formation of hydrates $HSO_5\bullet(H_2O)_x$ (x=1, 2, ...) can help to explain the observed nucleation in the atmosphere, as well as in the laboratory, starting from OH+SO_2.

5 Conclusions

We have investigated the effect of hydration on the $HSO_3+O_2\rightarrow SO_3+HO_2$ reaction, and especially on the stability of HSO_5 intermediate radicals, using advanced quantum chemical methods. Without hydration, the standard enthalpy and free energy of reaction are found to be very close to zero, in accordance with very recent high-level results. After hydration, the reaction becomes moderately endothermal. Hydration is found to stabilize the reactant form of HSO_5 (corresponding to a $HSO_3\bullet O_2$ complex) compared to the product form (corresponding to a $SO_3\bullet HO_2$ complex), and significantly increase the energy barrier for dissociation of HSO_5 into SO_3+HO_2. The dihydrated product complex was predicted to have at least a partial ion pair structure at several different levels of theory. Kinetic modeling indicates that HSO_3 hydration is likely to produce significant amounts of hydrated HSO_5 in atmospheric and laboratory conditions. The reactions of these hydrated complexes may help explain recent laboratory

observations of unexpectedly efficient nucleation from SO_2 oxidation initiated by OH radicals.

Acknowledgements. We thank the CSC centre for scientific computing for computer time. The authors are grateful to Hanna Vehkamäki, Martta Salonen and Ismael Kenty Ortega (Department of Physics, University of Helsinki, Finland) for helpful discussions.

References

Aaltonen, E. T. and Francisco, J. S: $HOSO_2$-H_2O Radical Complex and Its Possible Effects on the Production of Sulfuric Acid in the Atmosphere, J. Phys. Chem. A, 107, 1216–1221, 2003.

Ahlrichs, R., Bär, M., Häser, M., Horn, H., and Kölmel, C.: Electronic structure calculations on workstation computers: The program system Turbomole, Chem. Phys. Lett., 162, 165–169, 1989.

Alongi, K. S., Dibble, T. S., Shields, G. C., and Kirschner, K. N.: Exploration of the Potential Energy Surfaces, Prediction of Atmospheric Concentrations, and Prediction of Vibrational Spectra for the $HO_2 \ldots (H_2O)_n$ (n=1–2) Hydrogen Bonded Complexes, J. Phys. Chem. A, 110, 3686–3691, 2006.

Andersson, M. P. and Uvdal, P.: New Scale Factors for Harmonic Vibrational Frequencies Using the B3LYP Density Functional Method with the Triple-Z Basis Set 6-311+G(d,p), J. Phys. Chem. A, 109, 2937–2941, 2005.

Atkinson, R., Baulch, D. L., Cox, R. A., Hampson, R. F., Kerr, J. A., Rossi, M. J., and Troe, J. J.: Evaluated Kinetic, Photochemical and Heterogeneous Data for Atmospheric Chemistry: Supplement V. IUPAC Subcommittee on Gas Kinetic Data Evaluation for Atmospheric Chemistry, Phys. Chem. Ref. Data, 26, 521–1011, 1997.

Baboul, A. G., Curtiss, L. A., Redfern, P. C., and Raghavachari, K.: Gaussian-3 theory using density functional geometries and zero-point energies, J. Chem. Phys., 110, 7650–7658, 1999.

Ball, S. M., Hanson, D. R., Eisele, F. L. and McMurry, P. H.: Laboratory studies of particle nucleation: Initial results for H_2SO_4, H_2O, and NH_3 vapors, J. Geophys. Res. D, 104, 23709–23718, 1999.

Becke, A. D.: Density-functional thermochemistry. III. The role of exact exchange, J. Chem. Phys., 98, 5648–5652, 1993.

Benson, D. R., Young, L.-H., Kameel, F. R., and Lee, S.-H.: Laboratory-measured nucleation rates of sulfuric acid and water: binary homogeneous nucleation from the SO_2 + OH reaction, Geophys. Res. Lett., 35, L11801, doi:10.1029/2008GL033387, 2008.

Benson, S. W.: Thermochemistry and kinetics of sulphur-containing molecules and radicals, Chem. Rev., 78, 23–35, 1978.

Berndt, T., Böge, O., Stratmann, F., Heintzenberg, J., and Kulmala, M.: Rapid formation of sulfuric acid particles at near-atmospheric conditions, Science, 307, 698–700, 2005.

Berndt, T., Böge, O., and Stratmann, F.: Formation of atmospheric H_2SO_4/H_2O particles in the absence of organics: A laboratory study, Geophys. Res. Lett., 33, L15817, doi:10.1029/2006GL026660, 2006.

Berndt, T., Böge, O., and Stratmann, F.: Conference Abstract: Atmospheric H_2SO_4/H_2O Particle Formation: Mechanistic Investigations. 17th International Conference on Nucleation and Atmospheric Aerosols (ICNAA), Galway, Ireland, 69–72, 2007.

Berndt, T., Stratmann, F., Bräsel, S., Heintzenberg, J., Laaksonen, A., and Kulmala, M.: SO_2 oxidation products other than H_2SO_4 as a trigger of new particle formation. Part 1: Laboratory investigations, Atmos. Chem. Phys., 8, 6365–6374, 2008, http://www.atmos-chem-phys.net/8/6365/2008/.

Burkholder, J. B., Baynar, T., Ravishankara, A. R., and Lovejoy, E. R.: Particle nucleation following the O_3 and OH initiated oxidation of α-pinene and β-pinene between 278 and 320 K, J. Geophys. Res. 112, D10216, doi:10.1029/2006JD007783, 2007.

Curtiss, L. A., Raghavachari, K., Trucks, G. W., and Pople, J. A.: Gaussian-2 theory for molecular energies of first- and second-row compounds, J. Chem. Phys., 94, 7221–7230, 1991.

Das, T. N.: Reactivity and Role of SO_5^- Radical in Aqueous Medium Chain Oxidation of Sulfite to Sulfate and Atmospheric Sulfuric Acid Generation, J. Phys. Chem. A., 105, 9142–9155, 2001.

Davis, D., Ravishankara, A., and Fischer, S.: SO_2 Oxidation Via the Hydroxyl Radical: Atmospheric Fate of HSO_x Radicals, Geophys. Res. Lett., 6, 113–116, 1979.

Deegan, M. J. O. and Knowles, P. J.: Perturbative corrections to account for triple excitations in closed and open shell coupled cluster theories, Chem. Phys. Lett., 227, 321–326, 1994.

Dermota, T. E., Hydutsky, D. P., Bianco, N. J., and Castleman, A. W. Jr: Ultrafast Dynamics of the $SO_2(H2O)_n$ Cluster System, J. Phys. Chem. A, 109, 8254–8258, 2005.

Du, S., Francisco, J. S., Schenter, G. K., Iordanov, T. D., Garrett, B., Dupuis, M., and Li, J.: The OH radical-H_2O molecular interaction potential, J. Chem. Phys., 124, 224318, 2006.

Dunning, T. H. Jr., Peterson, K. A., and Wilson, A. K.: Gaussian basis sets for use in correlated molecular calculations. X. The atoms aluminum through argon revisited, J. Chem. Phys., 114, 9244–9253, 2001.

Fliegl, H., Glöß, A., Welz, O., Olzmann, M., and Klopper, W.: 2006. Accurate computational determination of the binding energy of the SO_3H_2O complex, J. Chem. Phys., 125, 054312, 2006.

Frisch, M. J., Trucks, G. W., Schlegel, H. B., Scuseria, G. E., Robb, M. A., Cheeseman, J. R., Montgomery, Jr., J. A., Vreven, T., Kudin, K. N., Burant, J. C., Millam, J. M., Iyengar, S. S., Tomasi, J., Barone, V., Mennucci, B., Cossi, M., Scalmani, G., Rega, N., Petersson, G. A., Nakatsuji, H., Hada, M., Ehara, M., Toyota, K., Fukuda, R., Hasegawa, J., Ishida, M., Nakajima, T., Honda, Y., Kitao, O., Nakai, H., Klene, M., Li, X., Knox, J. E., Hratchian, H. P., Cross, J. B., Bakken, V., Adamo, C., Jaramillo, J., Gomperts, R., Stratmann, R. E., Yazyev, O., Austin, A. J., Cammi, R., Pomelli, C., Ochterski, J. W., Ayala, P. Y., Morokuma, K., Voth, G. A., Salvador, P., Dannenberg, J. J., Zakrzewski, V. G., Dapprich, S., Daniels, A. D., Strain, M. C., Farkas, O., Malick, D. K., Rabuck, A. D., Raghavachari, K., Foresman, J. B., Ortiz, J. V., Cui, Q., Baboul, A. G., Clifford, S., Cioslowski, J., Stefanov, B. B., Liu, G., Liashenko, A., Piskorz, P., Komaromi, I., Martin, R. L., Fox, D. J., Keith, T., Al-Laham, M. A., Peng, C. Y., Nanayakkara, A., Challacombe, M., Gill, P. M. W., Johnson, B., Chen, W., Wong, M. W., Gonzalez, C., and Pople, J. A.: Gaussian 03, Revision C.02, Gaussian, Inc., Wallingford CT, USA, 2004.

Gleason, J. F., Sinha, A., and Howard, C. J.: Kinetics of the gas-phase reaction $HOSO_2 + O_2 \rightarrow HO_2 + SO_3$, J. Phys. Chem., 91, 719–724, 1987.

Gleason, J. F., and Howard, C. J.: Temperature dependence of the gas-phase reaction bisulfite radical + oxygen → hydroperoxo + sulfur trioxide, J. Phys. Chem. 92, 3414–3417, 1988.

Kanno, N., Tonokura, K., and Koshi, M.: Equilibrium constant of the HO_2-H_2O complex formation and kinetics of $HO_2 + HO_2$-H_2O: Implications for tropospheric chemistry, J. Geophys. Res., 111, D20312, doi:10.1029/2005JD006805, 2006.

Klopper, W., Tew, D. P., González-Garcia, N., and Olzmann, M.: Heat of formation of the $HOSO_2$ radical from accurate quantum chemical calculations, J. Chem. Phys., 129, 114308, 2008.

Knowles, P. J., Hampel, C., and Werner, H.-J.: Coupled cluster theory for high spin, open shell reference wave functions, J. Chem. Phys., 99, 5219–5227, 1993; erratum: J. Chem. Phys., 112, 3106, 2000.

Laaksonen, A., Kulmala, M., Berndt, T., Stratmann, F., Mikkonen, S., Ruuskanen, A., Lehtinen,

K. E. J., Dal Maso, M., Aalto, P., Petäjä, T., Riipinen, I., Sihto, S.-L., Janson, R., Arnold, F., Hanke, M., Ücker, J., Umann, B., Sellegri, K., O'Dowd, C. D., and Viisanen, Y.: SO_2 oxidation products other than H_2SO_4 as a trigger of new particle formation. Part 2: Comparison of ambient and laboratory measurements, and atmospheric implications, Atmos. Chem. Phys., 8, 7255–7264, 2008, http://www.atmos-chem-phys.net/8/7255/2008/.

Larson, L. J., Kuno, M., and Tao, F.-M.: Hydrolysis of sulfur trioxide to form sulfuric acid in small water clusters, J. Chem. Phys. 112, 8830–8838, 2000.

Lee, C., Yang, W., and Parr, R. G.: Development of the Colle-Salvetti correlation-energy formula into a functional of the electron density, Phys. Rev. B, 37, 785–789, 1988.

Li, W.-K. and McKee, M. L.: Theoretical Study of OH and H_2O Addition to SO_2, J. Phys. Chem. A, 101, 9778–9782, 1997.

Lovejoy, E. R. and Hanson, D. R,: Kinetics and Products of the Reaction $SO_3 + NH_3 + N_2$, J. Phys. Chem., 100, 4459–4465, 1996.

Majumdar, D., Kim, G.-S., Kim, J., Oh, K. S., Lee, J. Y., Kim, K. S., Choi, W. Y., Lee, S.-H., Kang M.-H., and Mhin, B. J.: Ab initio investigations of the $HOSO_2 + O_2 \rightarrow SO_3 + HO_2$ reaction, J. Chem. Phys., 122, 723–730, 2000.

Nagase S., Hashimoto, S., and Akimoto, H: $HOSO_2$, and $HOSO_4$, Radicals Studied by ab Initio Calculation and Matrix Isolation Technique, J. Phys. Chem., 92, 641–644, 1988.

Portmann, S.: MOLEKEL, Version 4.3.win32. Swiss Center for Scientific Computing (CSCS)/ETHZ, Switzerland, 2002.

Riipinen, I., Sihto, S.-L., Kulmala, M., Arnold, F., Dal Maso, M., Birmili, W., Saarnio, K., Teinilä, K., Kerminen, V.-M., Laaksonen A., and Lehtinen, K. E. J.: Connections between atmospheric sulphuric acid and new particle formation during QUEST III-IV campaigns in Heidelberg and Hyytiälä, Atmos Chem Phys. 7, 1899–1914, 2007.

Salonen, M., Kurtén, T., Vehkamäki, H., Berndt, T., and Kulmala, M.: Computational investigation of the possible role of some intermediate products of SO_2 oxidation in sulfuric acid – water nucleation, Atmos. Res., in press, 2009.

Solimannejad, M., Azimi, G., and Pejov, L: The HOO–SO_3 radical complex: ab initio and density-functional study, Chem. Phys. Lett., 391, 201–206, 2004.

Stockwell, W. R. and Calvert, J. G.: The mechanism of the HO-SO_2 reaction, Atmos. Environ., 17, 2231–2235, 1983.

Wavefunction, Inc: Spartan ' 02 Windows, Wavefunction, Inc., Irvine, CA, USA, http://www.

vavefun.com., 2002.
Wayne, R. P.: Chemistry of atmospheres, 3rd edition, Oxford University Press., Oxford, UK, 2000.
Weigend, F. and Häser, M: RI-MP2: first derivatives and global consistency, Theor. Chem. Acc., 97, 331–340, 1997.
Weigend, F., Häser, M., Patzelt, H., and Ahlrichs, R.: RI-MP2: Optimized auxiliary basis sets and demonstration of efficiency, Chem. Phys. Lett., 294, 143–152, 1998.
Werner, H.-J., Knowles, P. J., Lindh, R., Manby, F. R., Schütz, M., Celani, P., Korona, T., Rauhut, G., Amos, R. D., Bernhardsson, A., Berning, A., Cooper, D. L., Deegan, M. J. O. , Dobbyn, A. J., Eckert, F., Hampel, C., Hetzer, G., Lloyd, A. W., McNicholas, S. J., Meyer, W., Mura, M. E., Nicklass, A., Palmieri, P., Pitzer, R., Schumann, U., Stoll, H., Stone, A. J., Tarroni, R., and Thorsteinsson, T.: MOLPRO, version 2006.1, a package of ab initio programs, see http://www.molpro.net, 2006.
Young, L.-H., Benson, D. R., Kameel, F. R., and Lee, S.-H.: Laboratory studies of H_2SO_4/H_2O binary homogeneous nucleation from the SO_2 + OH reaction: evaluation of the experimental setup and preliminary results, Atmos. Chem. Phys., 8, 4997–5016, 2008, http://www.atmos-chem-phys.net/8/4997/2008/.

Table 1. Electronic energy change (ΔE_{elec}), enthalphy change (ΔH) and Gibbs free energy change (ΔG) for the reaction $HSO_3+O_2 \rightarrow SO_3+HO_2$, computed at various levels of theory. All values in kcal/mol. Enthalpies and Gibbs free energies correspond to 298 K and 1 atm reference pressure. A scaling factor of 0.967 has been used in the UB3LYP/6-311++G(3df,3pd) frequency calculations.

	ΔE_{elec}	ΔH	ΔG
MP2/6-31G(d,p)[a]	8.64	9.02	9.52
B3LYP/6-31G(d,p)[a]	9.29	9.94	10.58
MP2/TZ2P(f,d)++[a]	3.05	3.48	3.89
B3LYP/TZ2P(f,d)++[a]	4.52	4.82	5.39
MP2/cc-pVTZ[a]	2.35	2.77	3.26
MP2/cc-pVQZ[a]	0.58	–	–
MP2/cc-pV5Z[a]	−1.29	–	–
B3LYP/cc-pVQZ[a]	3.80	–	–
B3LYP/cc-pV5Z[a]	2.17	–	–
MP4(SDTQ)/6-31G(d,p)//HF/3-21G(d)[b]	11.9	12.3	12.8
Thermochemical prediction[c]	–	8±2	–
Thermochemical prediction[d]	–	0.9	–
CCSD(T), MP2-F12[e]		−2.3±0.7	
G2[f,g]	−3.98	−3.74	−3.16
G3B3[g]	−2.68	−2.44	−1.76
UCCSD/6-311++G(3df,3pd) //UB3LYP/6-311++G(3df,3pd)[g]	−1.33	−1.04	−0.46
UCCSD/aug-cc-pV(T+d)Z //UB3LYP/6-311++G(3df,3pd)[g]	−0.74	−0.46	0.13
UCCSD(T)/6-311++G(3df,3pd) //UB3LYP/6-311++G(3df,3pd)[g]	−1.24	−0.95	−0.37
UCCSD(T)/aug-cc-pV(T+d)Z //UB3LYP/6-311++G(3df,3pd)[g]	−0.61	−0.32	0.26

(a) Majumdar et al. (2000); (b) Nagase et al. (1988); a further extrapolation of the correlation energy beyond MP4 gave ΔH=10.6 kcal/mol; (c) Based on data by Benson, 1978; (d) Based on data by Atkinson et al. (1997); given by Li and McKee (1997); (e) Klopper et al. (2008); advanced multistep calculations involving MP2-F12/aug-cc-pwCV5Z and UCCSD(T)/cc-pV(T+d)Z calculations, together with anharmonic, hindered rotor and relativistic corrections. (f) Li and McKee (1997); (g) This study

Table 2. Electronic energy change (ΔE_{elec}), enthalpy change (ΔH) and Gibbs free energy change (ΔG) for the four individual steps of the overall reaction $HSO_3+O_2 \rightarrow SO_3+HO_2$, computed at various levels of theory. A scaling factor of 0.967 has been used in the UB3LYP/6-311++G(3df,3pd) frequency calculations. All values in kcal/mol. Enthalpies and Gibbs free energies correspond to 298 K and 1 atm reference pressure. HSO_5(R), HSO_5(TS) and HSO_5(P) correspond to the reactant, transition state and product complexes, respectively. (See the text and Fig. 1 for details.)

reaction, method	ΔE_{elec}	ΔH	ΔG
$HSO_3+O_2 \rightarrow HSO_5$(R)			
B3LYP/6-31G(d,p)[a]	−8.09	−6.26	5.06
MP2/6-31G(d,p)[a]	−3.67	−2.29	9.20
B3LYP/TZ2P++[a]	−6.08	−4.40	6.84
MP2/TZ2P++[a]	−6.28	−4.44	7.06
MP3/6-31G(d,p)//HF/3-21G(d)[b]	−1.2	3.2	14.4
Thermochemical prediction[c]	–	−16	–
G2[e]	−20.13	−18.56	−6.89
G3B3[e]	−14.76	−13.42	−2.67
UCCSD/6-311++G(3df,3pd) //UB3LYP/6-311++G(3df,3pd)[e]	−16.31	−14.63	−3.28
UCCSD/aug-cc-pV(T+d)Z //UB3LYP/6-311++G(3df,3pd)[e]	−17.60	−15.92	−4.57
UCCSD(T)/6-311++G(3df,3pd) //UB3LYP/6-311++G(3df,3pd)[e]	−16.01	−14.32	−2.98
UCCSD(T)/aug-cc-pV(T+d)Z //UB3LYP/6-311++G(3df,3pd)[e]	−17.33	−15.65	−4.30
HSO_5(R) → HSO_5(TS)			
B3LYP/6-31G(d,p)[a]	3.75	1.50	2.53
MP2/6-31G(d,p)[a]	2.10	0.46	1.27
B3LYP/TZ2P++[a]	4.20	1.60	2.65
MP2/TZ2P++[a]	1.87	0.29	1.03
G2[e]	6.49	4.06	4.79
G3B3[e]	6.65	1.94	3.43
UCCSD/6-311++G(3df,3pd) //UB3LYP/6-311++G(3df,3pd)[e]	10.46	7.89	8.80
UCCSD/aug-cc-pV(T+d)Z //UB3LYP/6-311++G(3df,3pd)[e]	10.72	8.16	9.07
UCCSD(T)/6-311++G(3df,3pd) //UB3LYP/6-311++G(3df,3pd)[e]	6.49	3.92	4.83
UCCSD(T)/aug-cc-pV(T+d)Z //UB3LYP/6-311++G(3df,3pd)[e]	6.73	4.16	5.07

(a) Majumdar et al. (2000); (b) Nagase et al. (1997); (c) Based on data by Benson (1978); (d) Solimannejad et al. (2004); (e) This study

ACPD
9, 2823–2853, 2009

Table 2. Continued.

reaction, method	ΔE_{elec}	ΔH	ΔG
$HSO_5(TS) \rightarrow HSO_5(P)$			
B3LYP/6-31G(d,p)[a]	−2.05	0.56	−0.64
MP2/6-31G(d,p)[a]	−2.28	−0.37	−2.11
B3LYP/TZ2P++[a]	−3.84	−1.05	−2.34
G2[e]	−2.69	−0.09	−3.50
G3B3[e]	−4.82	−2.08	−3.34
UCCSD/6-311++G(3df,3pd) //UB3LYP/6-311++G(3df,3pd)[e]	−5.70	−2.98	−4.33
UCCSD/aug-cc-pV(T+d)Z //UB3LYP/6-311++G(3df,3pd)[e]	−4.90	−2.18	−3.53
UCCSD(T)/6-311++G(3df,3pd) //UB3LYP/6-311++G(3df,3pd)[e]	−3.84	−1.13	−2.48
UCCSD(T)/aug-cc-pV(T+d)Z //UB3LYP/6-311++G(3df,3pd)[e]	−3.04	−0.33	−1.68
$HSO_5(P) \rightarrow SO_3 + HO_2$			
B3LYP/6-31G(d,p)[a]	15.67	14.14	3.63
MP2/6-31G(d,p)[a]	12.51	9.39	1.16
B3LYP/TZ2P++[a]	10.93	9.36	−1.05
B3LYP/6-311++G(2df,2p)[d]	11.20	–	–
MP2/6-311++G(2df,2p)[d]	12.19	–	–
G3[d]	11.51	11.54	2.08
G3MP2 [d]	10.25	10.28	4.58
G2[e]	12.35	10.85	2.44
G3B3[e]	12.68	11.13	0.82
UCCSD/6-311++G(3df,3pd) //UB3LYP/6-311++G(3df,3pd)[e]	10.22	8.67	−1.65
UCCSD/aug-cc-pV(T+d)Z //UB3LYP/6-311++G(3df,3pd)[e]	11.03	9.49	−0.83
UCCSD(T)/6-311++G(3df,3pd) //UB3LYP/6-311++G(3df,3pd)[e]	12.12	10.58	0.25
UCCSD(T)/aug-cc-pV(T+d)Z //UB3LYP/6-311++G(3df,3pd)[e]	13.04	11.50	1.17

(a) Majumdar et al. (2000); (b) Nagase et al. (1997); (c) Based on data by Benson (1978); (d) Solimannejad et al. (2004); (e) This study

ACPD
9, 2823–2853, 2009

Table 3. Electronic energy change (ΔE_{elec}), enthalphy change (ΔH) and Gibb's free energy change (ΔG) for hydration reactions of various molecules: $X+n(H_2O) \rightarrow X\bullet(H_2O)_n$. A scaling factor of 0.967 has been used in the UB3LYP/6-311++G(3df,3pd) frequency calculations. All values in kcal/mol. Enthalpies and Gibbs free energies correspond to 298 K and 1 atm reference pressure. HSO_5(R), HSO_5(TS) and HSO_5(P) correspond to the reactant, transition state and product complexes, respectively. (See the text and Fig. 1 for details.) When multiple literature values exist for some parameter, only the highest-level ones are given.

cluster, method	ΔE_{elec}	ΔH	ΔG
$SO_2\bullet H_2O$, G2[a]	−3.46	−3.51	3.62
$SO_2\bullet H_2O$, G3B3[h]	−4.55	−3.06	4.44
$SO_2\bullet H_2O$, UCCSD(T)/aug-cc-pV(T+d)Z //UB3LYP/6-311++G(3df,3pd)[h]	−4.51	−3.19	3.23
$OH\bullet H_2O$, RCCSD(T)/aug-cc-pVTZ[b]	−5.88	–	–
$OH\bullet H_2O$, G3B3[h]	−5.59	−4.13	2.14
$OH\bullet H_2O$, UCCSD(T)/aug-cc-pVTZ //UB3LYP/6-311++G(3df,3pd)[h]	−5.88	−4.52	1.70
$OH\bullet(H_2O)_2$, mTTM potential[b]	−14.86	–	–
$OH\bullet(H_2O)_2$, G3B3[h]	−14.37	−10.62	6.28
$HSO_3\bullet H_2O$, UB3LYP/6-311++G(3df,3pd)[c]	−10.90	–	–
$HSO_3\bullet H_2O$, G3B3[h]	−12.29	−10.51	−1.06
$HSO_3\bullet H_2O$, UCCSD(T)/aug-cc-pV(T+d)Z //UB3LYP/6-311++G(3df,3pd)[h]	−12.56	−10.94	−1.93
$HSO_3\bullet(H_2O)_2$, G3B3[h]	−24.10	−20.76	−2.30
$HSO_3\bullet(H_2O)_2$, UCCSD(T)/aug-cc-pV(T+d)Z //UB3LYP/6-311++G(3df,3pd)[h]	−24.45	−21.36	−3.00
HSO_5(R)$\bullet H_2O$, G3B3[h]	−17.28	−15.28	−4.88
HSO_5(R)$\bullet H_2O$, UCCSD(T)/aug-cc-pV(T+d)Z //UB3LYP/6-311++G(3df,3pd)[h]	−14.35	−12.91	−3.78
HSO_5(R)$\bullet(H_2O)_2$, G3B3[h]	−29.09	−26.11	−6.07

(a) Li and McKee, 1997; (b) Du et al., 2006; (c) Aaltonen and Fransisco, 2003; (d) Fliegl et al., 2006; advanced multistep calculations involving RI-MP2-R12/def2-QZVPP and CCSD(T)/aug-cc-pV(Q+d)Z energies together with B3LYP/cc-pVTZ frequencies. (e) Larsen et al., 2000; (f) Kanno et al., 2006; (g) Alongi et al., 2006; (h) This work

ACPD
9, 2823–2853, 2009

Table 3. Continued.

cluster, method	ΔE_{elec}	ΔH	ΔG
$HSO_5(P)\bullet H_2O$, G3B3[h]	−11.69	−10.03	−0.29
$HSO_5(P)\bullet H_2O$, UCCSD(T)/aug-cc-pV(T+d)Z //UB3LYP/6-311++G(3df,3pd)[h]	−11.12	−9.72	−0.37
$HSO_5(P)\bullet (H_2O)_2$, G3B3[h]	−27.71	−24.60	−3.48
$SO_3\bullet H_2O$, RI-MP2-R12, CCSD(T)[d]	−9.8±0.2	−8.3±1.0	–
$SO_3\bullet H_2O$, G3B3[h]	−10.32	−8.51	−0.38
$SO_3\bullet H_2O$, UCCSD(T)/aug-cc-pV(T+d)Z //UB3LYP/6-311++G(3df,3pd)[h]	−9.76	−8.12	−0.59
$SO_3\bullet (H_2O)_2$, B3LYP/6-311++G(d,p)[e]	−21.86	–	–
$SO_3\bullet (H_2O)_2$, MP2/6-311++G(d,p)[e]	−21.87	–	–
$SO_3\bullet (H_2O)_2$, G3B3[h]	−22.26	−18.42	−0.03
$SO_3\bullet (H_2O)_2$, UCCSD(T)/aug-cc-pV(T+d)Z //UB3LYP/6-311++G(3df,3pd)[h]	−22.31	−18.78	−1.07
$HO_2\bullet H_2O$, experimental[f]		−7.4±1	
$HO_2\bullet H_2O$, G3[g]	−9.14	−7.42	−0.53
$HO_2\bullet H_2O$, G3B3[h]	−8.88	−6.77	2.33
$HO_2\bullet H_2O$, UCCSD(T)/aug-cc-pVTZ //UB3LYP/6-311++G(3df,3pd)[h]	−9.48	−7.68	0.44
$HO_2\bullet (H_2O)_2$, G3[g]	−20.64	−16.98	−0.47
$HO_2\bullet (H_2O)_2$, G3B3[h]	−20.33	−16.44	2.33
$HO_2\bullet (H_2O)_2$, UCCSD(T)/aug-cc-pVTZ //UB3LYP/6-311++G(3df,3pd)[h]	−21.12	−17.59	0.62

(a) Li and McKee, 1997; (b) Du et al., 2006; (c) Aaltonen and Fransisco, 2003; (d) Fliegl et al., 2006; advanced multistep calculations involving RI-MP2-R12/def2-QZVPP and CCSD(T)/aug-cc-pV(Q+d)Z energies together with B3LYP/cc-pVTZ frequencies. (e) Larsen et al., 2000; (f) Kanno et al., 2006; (g) Alongi et al., 2006; (h) This work

ACPD
9, 2823–2853, 2009

Table 4. Electronic energy change (ΔE_{elec}) and Gibb's free energy change (ΔG) for various reaction pathways corresponding to Reactions (2a), (2c)+(2d) and (2f), but including the effects of hydration. All values in kcal/mol. "CCSD(T)" corresponds to UCCSD(T)/aug-cc-pV(T+d)Z single-point energies and UB3LYP/6-311++G(3df,3pd) geometries and frequencies. A scaling factor of 0.967 has been used in the UB3LYP/6-311++G(3df,3pd) frequency calculations. Gibbs free energies correspond to 298 K and 1 atm reference pressure.

Reaction	CCSD(T) ΔE_{elec}	CCSD(T) ΔG	G3B3 ΔE_{elec}	G3B3 ΔG
$HSO_3{\bullet}H_2O + O_2 \rightarrow SO_3{\bullet}H_2O + HO_2$	2.19	1.60	−0.71	−1.08
$HSO_3{\bullet}H_2O + O_2 \rightarrow SO_3 + HO_2{\bullet}H_2O$	2.48	2.64	0.74	1.63
$HSO_3{\bullet}(H_2O)_2 + O_2 \rightarrow SO_3{\bullet}H_2O + HO_2{\bullet}H_2O$	4.61	3.12	2.22	2.48
$HSO_3{\bullet}(H_2O)_2 + O_2 \rightarrow SO_3{\bullet}(H_2O)_2 + HO_2$	1.53	2.20	−0.84	0.51
$HSO_3{\bullet}(H_2O)_2 + O_2 \rightarrow SO_3 + HO_2{\bullet}(H_2O)_2$	2.73	3.89	1.09	2.87
$HSO_5(R){\bullet}H_2O \rightarrow\rightarrow HSO_5(P){\bullet}H_2O$	6.91	6.81	5.00	4.67
$HSO_5(R){\bullet}(H_2O)_2 \rightarrow\rightarrow HSO_5(P){\bullet}(H_2O)_2$	–	–	1.36	1.36
$HSO_5(P){\bullet}H_2O \rightarrow SO_3{\bullet}H_2O + HO_2$	14.41	0.95	14.04	0.73
$HSO_5(P){\bullet}H_2O \rightarrow SO_3 + HO_2{\bullet}H_2O$	14.69	1.98	15.49	3.44
$HSO_5(P){\bullet}(H_2O)_2 \rightarrow SO_3{\bullet}H_2O + HO_2{\bullet}H_2O$	–	–	21.19	6.24
$HSO_5(P){\bullet}(H_2O)_2 \rightarrow SO_3{\bullet}(H_2O)_2 + HO_2$	–	–	18.13	4.26
$HSO_5(P){\bullet}(H_2O)_2 \rightarrow SO_3 + HO_2{\bullet}(H_2O)_2$	–	–	20.06	6.62

ACPD
9, 2823–2853, 2009

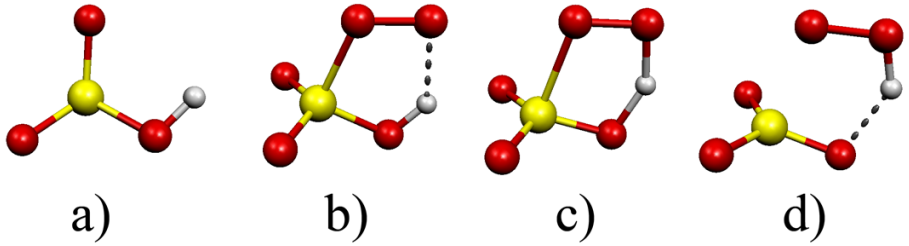

Fig. 1. Minimum – energy structures (at the G3B3 level) of **(a)** HSO_3, **(b)** HSO_5(R), **(c)** HSO_5(TS) and **(d)** HSO_5(P). Dashed lines correspond to hydrogen bonds. Color coding: yellow=sulfur, red=oxygen, white=hydrogen.

ACPD
9, 2823–2853, 2009

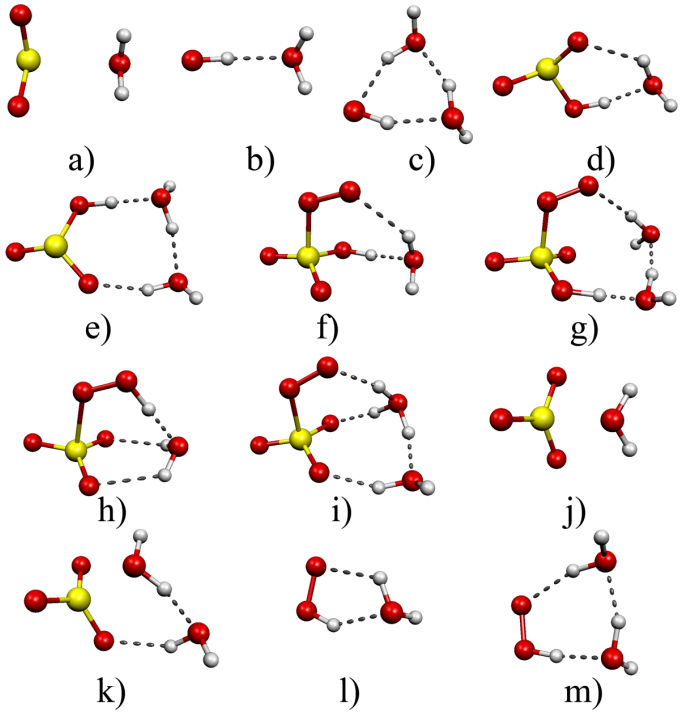

Fig. 2. Minimum – energy structures (at the G3B3 level) of **(a)** $SO_2 \bullet H_2O$, **(b)** $OH \bullet H_2O$, **(c)** $OH \bullet (H_2O)_2$, **(d)** $HSO_3 \bullet H_2O$, **(e)** $HSO_3 \bullet (H_2O)_2$, **(f)** $HSO_5(R) \bullet H_2O$, **(g)** $HSO_5(R) \bullet (H_2O)_2$, **(h)** $HSO_5(P) \bullet H_2O$, **(i)** $HSO_5(P) \bullet (H_2O)_2$, **(j)** $SO_3 \bullet H_2O$, **(k)** $SO_3 \bullet (H_2O)_2$, **(l)** $HO_2 \bullet H_2O$, **(m)** $HO_2 \bullet (H_2O)_2$. Dashed lines correspond to hydrogen bonds. Color coding: yellow=sulfur, red=oxygen, white=hydrogen.

ACPD
9, 2823–2853, 2009